



Strengthening of Lap-Spliced RC Beams Using Near-Surface Mounting Method

Seyed Roohollah Mousavi¹ · Mohammad Reza Sohrabi¹ · Yaser Moodi¹ · Ebrahim Gholamhosseini¹

Received: 24 April 2020 / Accepted: 28 December 2020
© Shiraz University 2021

Abstract

An adequate bond between concrete and reinforcement along lap-splice length is necessary to prevent bond failure in lap-splice zone. Sometimes, lap splice has insufficient bond due to such various reasons as design and construction errors and needs strengthening. NSM and FRP confinement are highly promising methods compared to other available methods. NSM and NSM–CFRP confinement methods used for this purpose, and bonded length and concrete cover were considered as variables. The results reveal that the specifications of lap-spliced RC beams (load-bearing capacity, energy dissipation capacity, and ductility) are increased using strengthening methods. In the NSM, the lap-spliced beam's strength would be increased, while CFRP leads to more ductility. Besides, load-bearing capacity and ductility led to more values when the concrete cover is increased.

Keywords RC beam · Strengthening · NSM · Confinement · Lap-spliced

1 Introduction

Providing adequate bonds between concrete and rebar along lap-splice length is essential for RC structures' design. It is necessary to prevent splitting/pullout failure in lap-splice zone as the most vulnerable part of member. Different methods were investigated for strengthening such structures. When FRP fiber-reinforced polymers entered building industry, several problems were solved for strengthening. (Fakharifar et al. 2016) used FRP sheets as stirrup to improve RC structures' behavior. They revealed that FRP stirrups improved strength, stiffness, and energy dissipation. (Siddika et al. 2019) reported that FRPs have superior strength development and durability performance. The mentioned study also provided a straightforward perspective of improving

RC beams' application and performances by strengthening FRP. (Kheyroddin et al. 2011) used FRP sheets to strengthen RC coupled beam and have shown that FRP could significantly improve these beams' strength and deformation capacity. Externally bonded reinforcement strengthening method with FRP sheets, called EBR, can be considered a very common beam reinforcement method due to sticking FRP sheets on the outer surface of RC beams using strong adhesives. Experimental tests showed if strengthening is done using EBR method, three failure modes are possible: flexural, shear, and FRP debonding (Mostofinejad and Moghaddasi 2014). In 2017, (Al-Rousan and Issa 2017) assessed exterior retrofitting effect of RC beams exposed to severe environmental conditions using the CFRP sheet. (Lamanna et al. 2004) used a mechanically fastened (MF) system to attach FRP strips for concrete. They indicated that non-fasteners specimens had a lower strengthening effect compared to the specimens which had the fasteners at the moment. (Nardone et al. 2011) presented an analytical model for members strengthened by MF-FRP strips. This model estimates experimental results well. (Hassan and Rizkalla 2002) investigated five different strengthening approaches. They concluded that NSM method by CFRP strips was three times efficient rather than EBR method. Therefore, NSM performed better than EBR because premature debonding failure was prevented; however, differences could be due

✉ Seyed Roohollah Mousavi
s.r.mousavi@eng.usb.ac.ir

Mohammad Reza Sohrabi
sohrabi@hamoon.usb.ac.ir

Yaser Moodi
y.moodi.civil@gmail.com

Ebrahim Gholamhosseini
gh.ebram@gmail.com

¹ Civil Engineering Department, University of Sistan and Baluchestan, Zahedan, Iran

to applied reinforcement amount. (El-Hacha and Rizkalla 2004) concluded that RC beams strengthened with CFRP strips using NSM method led to more load-bearing capacities compared to EBR in the same condition. (Obaidat et al. 2020) used NSM–CFRP strips for strengthening the RC beam subjected to pure torsional loading in the laboratory. (Haddad and Almomani 2019) used NSM method to strengthen RC beams which showed NSM CFRP strips to increase residual flexural capacity.

Studies about strengthening RC structures using FRP materials are different (Al-Mahmoud et al. 2009; Moodi et al. 2017, 2018; Hassan and Rizkalla 2003; Hashemi et al. 2009). The effect of FRP on retrofitting the columns with lap splices were investigated by ElGawady et al. (2010), Youm et al. (2007), ElSouri and Harajli (2011), and Bournas and Triantafillou (2011), while a few studies investigated the effect of FRP on strengthening lap-spliced RC beams such as Hamad et al. (2004a, b). In 2002, they examined GFRP wrap's effects on the bond strength using seven lapped RC beams which have high-strength concrete (Hamad et al. 2004a). Considering GFRP array and number of layers as their variables, they showed using one and two layers of GFRP wrap increased the bond strength by 8% and 33%, respectively. In another study about normal-strength RC beams, they showed that CFRP wrap effects on normal and high-strength concretes were the same; using one and two layers of this wrap on normal concrete increased bond strength by 11% and 34%, respectively (Hamad et al. 2004b).

In 2013, the effects of two strengthening methods (NSM with steel bars and CFRP and EBR with steel plate and laminated CFRP) on lap-spliced beams were investigated. The results showed: i) the flexural capacities of strengthened beams increased 73–91% compared to lap-spliced beams and 27–40% compared to beams without lap splice and ii) the ductility in NSM method was more than that in EBR method (Allam 2013). Garcia et al. (2014, 2015) investigated the confinement effects of lap-splice zone using stirrups (internally) and CFRP confinement (externally). They showed that stirrups increased bond strength by 14% and rebar slip by 2790% (preserving bond strength), while CFRP confinement increased the former by 65% and the latter by 14,000%. A study about strengthening columns with lap-spliced bars by FRP confinement was done by Anagnostou et al. (2019). Garcia et al. (2017) tried to investigate FRP effectiveness in controlling bond-splitting failures.

While studying the effects of the NSM method on strengthening lap-spliced RC beams is limited, none was found on the effects of combining NSM-FRP confinement method for mentioned task. This study investigated NSM effects and combining NSM–CFRP confinement strengthening methods on lap-spliced RC beams and short lap-splice length. In addition to strengthening method, concrete cover (bottom) and NSM rebar length were considered variables.

Results showed that strengthening methods increase the load-bearing capacity, ductility, and energy absorption capacity of the lap-spliced RC beams.

2 Experimental Program

2.1 Details of Specimens

Eight lap-spliced RC beams 150×200 mm in the cross-sectional area and 2300 mm in length were manufactured which were tested under four-point bending. According to this study's objectives, longitudinal and transverse bars were designed so that bending failure, due to insufficient lap-splice length, can occur. Also, to show the effect of retrofitting methods, tensile bars were spliced in the mid-span with lap-splice length shorter than the required length. Tensile bars include two 12-mm-diameter steel bars, and compressive bars include two 8-mm-diameter continuous bars. To consider the bond failure in beams and create the need to strengthen, the lap-splice length (L_d) was taken to be 20 cm (insufficient overlapping). To prevent shear failure, 8-mm-diameter stirrups were placed through beam length with 85-mm center-to-center distance (three stirrups in lap-spliced zone). Figure 1 shows the specimens' dimensions, the distance among supports, and clear bending span.

The concrete cover (bottom), strengthening method (NSM and combination of NSM–CFRP confinement), and NSM rebar bond length in concrete were variables. Specimens included two types: i) with 25-mm concrete cover (bottom) and ii) with 40-mm concrete cover (bottom); each type contained control specimens, specimens which retrofitted by NSM technique which had a variable length of the bond (800 and 1300 mm) and with NSM–CFRP confinement combination method. The specimens are labeled with CaLbWc where a indicates the bottom concrete cover (mm), b shows the NSM-GFRP rebar bond length (mm), and c represents the presence or absence of the CFRP wrap ($c = N$ if CFRP wrap does not exist and $c = R$ if it does). The width of CFRP layers was 50 mm in specimens strengthened with the NSM–CFRP method, and those are discontinuously used at two ends of lap-splice zones. The specimen details are listed in Table 1. Strengthening methods arrangement (NSM bars and CFRP wrap) for the retrofitted specimens is shown in Fig. 2.

3 Specifications of Materials

All beams were made of ready-made concrete, and the compressive strength of 28-day standard concrete cylinders, cured under the same conditions as beams, was 32 MPa. AIII (S340) and AII (S400) steel bars were used

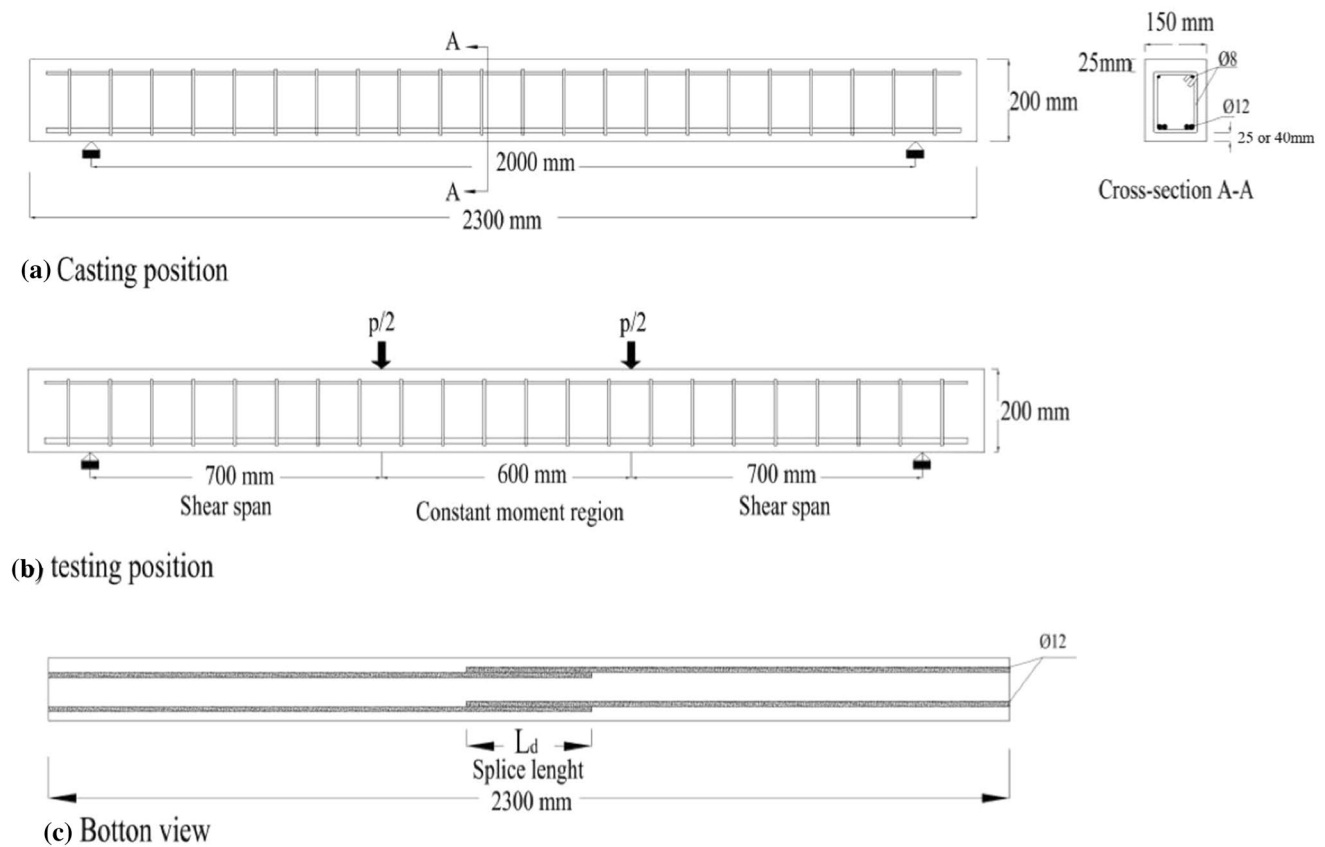


Fig. 1 Specimen details

Table 1 Details of specimens

Specimen	Bottom concrete cover C_y (mm)	NSM-GFRP rebar bond length (mm)	CFRP layers
C25ctrl	25	—	—
C25L800WN	25	800	—
C25L800WR	25	800	2
C25L1300WN	25	1300	—
C40ctrl	40	—	—
C40L800WN	40	800	—
C40L800WR	40	800	2
C40L1300WN	40	1300	—

as longitudinal reinforcements and stirrups, respectively. Due to the tensile test by DIN EN 1002 Code (DIN 1991), the steel bars' mechanical properties are provided in Table 2.

FRP bars used in specimens were 8 mm in diameter made of glass, and their mechanical specification was obtained using tensile tests following ACI440.3R Standard (ACI440 2004). The elasticity modulus and the ultimate stress of GFRP bars were 45,320 and 990 MPa, respectively; some

mechanical characteristics of epoxy adhesive used to connect GFRP bars are provided in Table 3.

In this study, carbon fibers were unidirectional fibers and had a thickness of 0.11 mm (a product of the Quantum Co.). Ultimate strength and elastic modulus of CFRP wraps were 4950 and 240,000 MPa, respectively, due to factory specifications. Some mechanical characteristics of adhesive used to connect the CFRP sheet are given in Table 3.

4 Specimen Setup

After 28 days of curing, a gear cutter was used to create grooves with the dimensions of 16×16 mm and intended lengths (800 and 1300 mm) on the tensile surface of beams (Fig. 3). They were cleaned of any dust by a strong air pump to facilitate adhesive sticking inside them. GFRP bars were cut with the desired length; epoxy adhesives were mixed with a ratio of 1: 3, half the groove had filled with the adhesive, bars were placed inside grooves, empty groove part had filled with adhesive, and the surface was smoothed. For specimens with CFRP confinement, beams corners were first rounded with a radius of 15 mm to

Fig. 2 Strengthening methods arrangement: **a** NSM method with 800 mm bond length, **b** NSM method with 1300 mm bond length and **c** NSM–CFRP confinement combination method

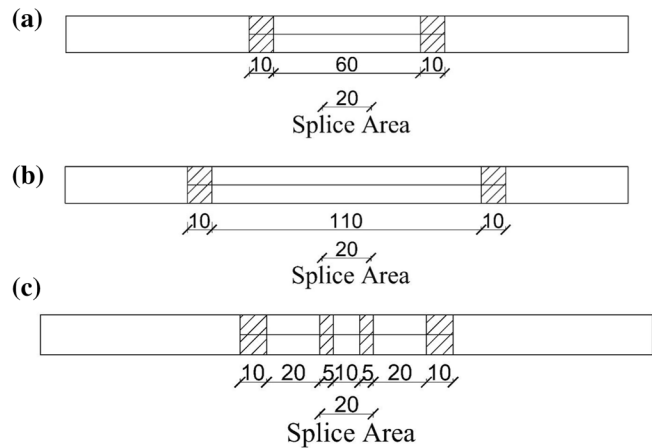


Table 2 Mechanical properties of steel reinforcement

Bar type	Yielding stress (MPa)	Ultimate stress (MPa)
A-II bar with diameter of 8 mm	393	556
A-III bar with diameter of 12 mm	464	701

prevent stress concentrations. Then, CFRP sheets were cut to desired size; to stick the sheets on beams, use was made of wet lay-up method. The surfaces were first covered with epoxy resin with a spatula. Then, CFRP sheets were manually pressed on the surface.

All specimens strengthened with GFRP bars were made of 10-cm-wide CFRP sheets at the end of bars as retainers to prevent their ends from the debonding failure.

5 Loading Process

A four-point bending with simple supports and a span length of 2000 mm were applied to the specimens. In this case, bending was performed on the beam as follows: The load was applied to the beam by a jack such that a spreader loading beam was placed between beam and jack. Net bending length of beams was 600 mm. The load cell located between the jack and the spreader was used to measure the beams' load. An LVDT measured midspan deflection, and a data logger recorded the general information (applied load and midspan deflection).

6 Results of Tests

All specimen test results, including load-carrying capacity (P_{max}), final deflection (Δ_u), the percentage increase in load-carrying capacity compared to control specimen, ductility index (i), initial stiffness (K_0), and specimens' energy dissipation capacities, are given in Table 4. Findings are provided in the following sections.

Table 3 The mechanical properties of epoxy adhesives

	EPR 301	EPR 3301
Density (at 25 °C)	1.6 kg/l (mixed)	1.6 kg/l (mixed)
Bonding strength	> 1.8 MPa (concrete failed)	> 3.5 MPa (concrete failed)
Compressive strength	Minimum 60 MPa (7 days)	Minimum 95 MPa (7 days)
Flexural strength	> 25 MPa	> 30 MPa

Fig. 3 Groove in beams



Table 4 Summary results

Specimen	Maximum load-carrying capacity (kN)	Ultimate displacement (mm)	Percentage of increasing (%)	K_0 (kN/mm)	Ductility index	Energy dissipation capacity (kN.mm)	Failure modes
C25ctrl	36.44	15.84	-	4.27	1.87	408.25	Splitting of concrete cover
C25L800WN	43.71	26.4	19.95	4.72	2.88	918.35	Debonding of the GFRP bars
C25L800WR	46	36.6	26.23	4.46	3.62	1398.24	Rupturing the CFRP sheet
C25L1300WN	49.81	30.3	36.69	4.43	2.79	1184.52	Debonding of GFRP bars along with the concrete cover
C40ctrl	38.74	19.1	—	5.39	2.57	549.32	Splitting of concrete cover
C40L800WN	46.26	38.1	19.41	3.98	3.27	1401.95	Rupturing the end confining CFRP laminate and debonding of GFRP bars
C40L800WR	48.74	37.3	25.81	4.66	3.61	1497.61	Rupturing the CFRP sheet
C40L1300WN	55.39	41.3	46.76	3.88	2.98	1756.6	Debonding of GFRP bars along with the concrete cover

7 Failure Types

Due to specimen C25ctrl, micro-cracks were formed under loading, and when the loading was raised, the number and width of cracks also increased. It is noteworthy that the largest crack is visible at the end of lap-splice zone; this specimen's failure mode was concrete cover splitting (Fig. 4a).

In specimen C25L800WN, the first micro-cracks were observed at a load of 14 kN. Major cracks were created at the end of GFRP bars area. The beam failure occurred, at a load of almost 43 kN, when GFRP bars and epoxy adhesive were debonded. The main reason for GFRP bars' debonding is due to no sufficient bond strength between concrete and epoxy (Fig. 4b). In specimen C25L800WR, strengthened in lap-splice zone, using the combination of NSM-GFRP and CFRP confinement methods, the first cracks occurred in concrete surface outside the constant moment area at a load greater than 20 kN. When the loading continued, GFRP bars were released by rupturing CFRP laminate and failure occurred at a load of about 46 kN (Fig. 4c).

In specimen C25L1300WN, the first cracks were created in midspan (at the end of lap-splice zone). Outside the strengthened area, cracks occurred at a load above 30 kN, and in the epoxy adhesive, they were visible at a 40 kN load. Horizontal cracks occurred through NSM bars at a 44 kN load, and the beam failed when GFRP bars, epoxy adhesive, and bottom concrete cover debonded in lap-splice zone (Fig. 4d). Debonding of GFRP bars along

with the concrete cover is an indication of a better GFRP bar-concrete bonding. Rupturing was observed in GFRP bars after the failure.

In specimen C40ctrl with a bottom concrete cover of 40 mm, first cracks were formed at a load of about 10 kN, and when the loading increased, the number and width of cracks increased (Fig. 4e). The failure mode of this specimen was concrete cover splitting at a load of 38 kN.

When the loading was applied to specimen C40L800WN, initial cracks were formed at a load of about 10 kN. First, cracks in the epoxy resin were observed at a load of 42 kN. When loading increased, the number of cracks in the epoxy resin of CFRP laminate also increased. Most cracks grew in the region between the end of GFRP bars and lap-splice zone. Finally, by increased loading and growth of cracks, GFRP bars were released by rupturing the end confining CFRP laminate (Fig. 4f).

In specimen C40L800WR, the first cracks occurred at a 14 kN load, and most cracks were observed outside strengthening area when loading began. As it continued, some cracks were formed in CFRP laminate at a load of 45 kN. Finally, GFRP bars were released together with the concrete by rupturing CFRP laminate (Fig. 4g).

In specimen C40L1300WN, first cracks occurred on the concrete surface at 8 kN load; cracks started in the midspan in lap-splice area and spread uniformly. Horizontal cracks began in side faces of beam at a 41 kN load. This specimen failed, similar to specimen C25L1300, by debonding GFRP

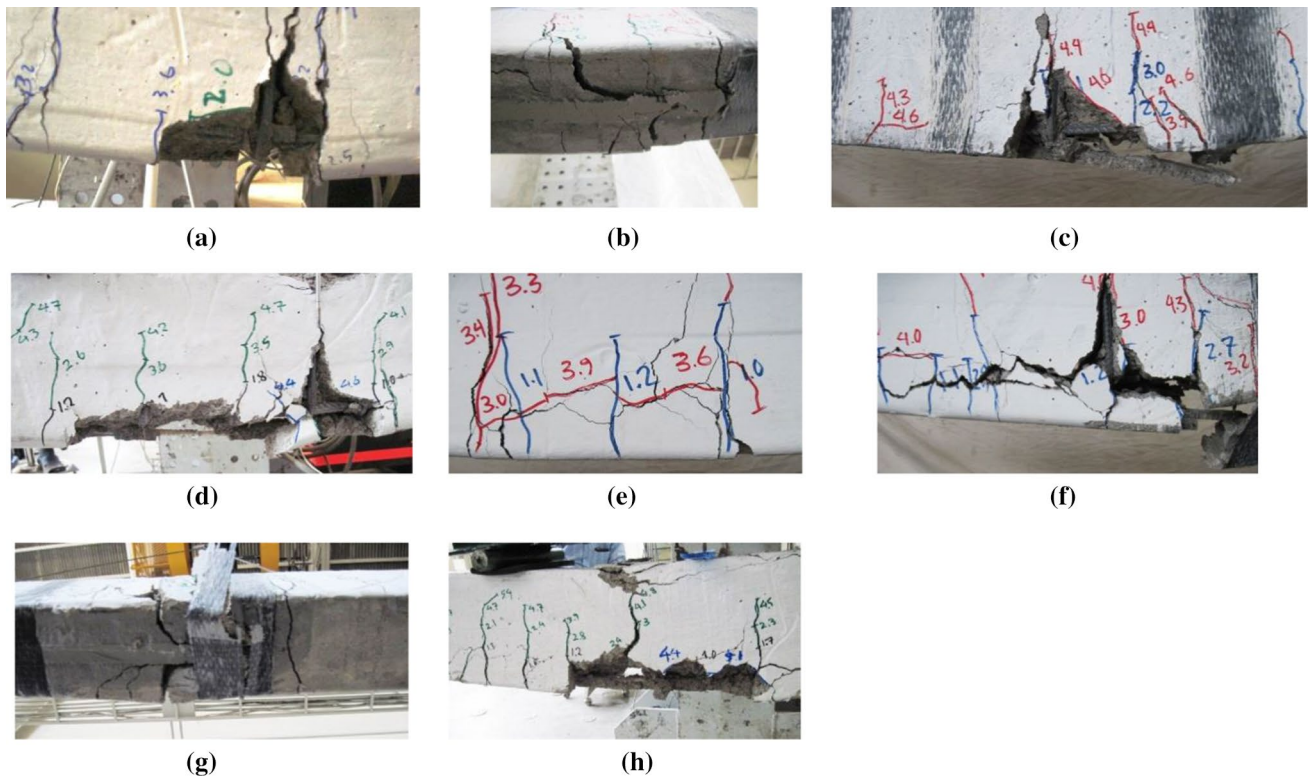


Fig. 4 Propagation and position of cracks

bars and bottom concrete cover in lap-splice zone with a loud sound (Fig. 4h).

8 Load–Deflection Diagram (Maximum Load-Carrying Capacity and Initial Stiffness)

Figure 5 shows load–midspan deflection diagram for different bottom concrete covers. As shown, strengthening methods have increased the flexural strength of lap-spliced beams by an average of 29% compared with the control specimens. NSM strengthening method with a bond length of 1300 mm causes the highest increase in the flexural strength. The NSM–CFRP confinement combined method increases this strength by an average ignorable amount of approximately 5% compared to specimens strengthened by NSM method with 800 mm long. However, an increase in NSM bars' bond length will increase the flexural strength by about 17%. Consequently, an increase in the bond length would be improved the flexural strength compared to confining the lap-splice zone.

It should be noted that the concrete cover has no effects on the strength of specimens strengthened by NSM method with 800 mm bond length and NSM–CFRP confinement combined method. When the bond length of NSM bar is

1300 mm, concrete cover in NSM method causes an increase of about 27% in specimen strength. Table 4 and Fig. 5 show that strengthening methods do not considerably affect the initial stiffness; however, they reduce it in some cases.

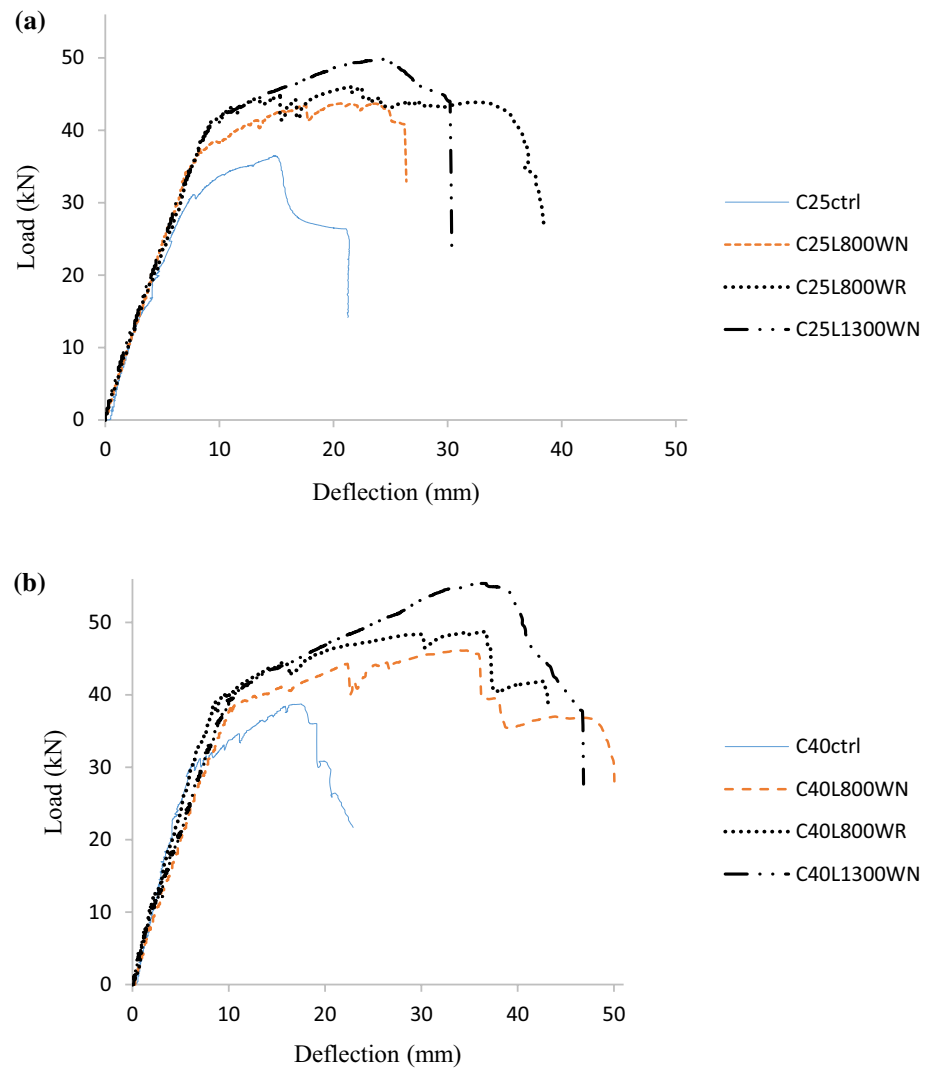
9 Ultimate Deflection and Ductility Index

Ultimate deflection (Δ_u) is the displacement corresponding to 85% of the maximum force on the load–displacement curve's descending branch. Cohn and Barlett (1982) method is also performed to calculate ductility index (μ). This index's calculating process has been explained in the study of (Moodi et al. 2020). This index is defined as the ratio of ultimate deflection to displacement due to maximum force in elastic behavior region (Δ_y) as follows:

$$\eta = \frac{\Delta_u}{\Delta_y}. \quad (1)$$

The ductility index of all specimens was calculated as shown in Table 4. Strengthening methods increase final displacement; CFRP confinement effect on increasing final displacement is higher when the concrete cover is lower, and the bond length of NSM bar does so when concrete cover is more.

Fig. 5 The load–midspan deflection diagram: **a** beams with concrete cover of 25 mm and **b** beams with concrete cover of 40 mm



Beams (both strengthened and not strengthened) with more concrete covers have more ductility index. Strengthening methods would increase beam ductility. NSM bar with a length of 800 mm increases ductility by 54 and 27% for concrete covers of 25 and 40 mm, respectively, compared to control specimens with similar concrete covers. However, it was obvious that an increase in NSM bar bond length might slightly descend ductility. Before debonding of GFRP bars, the reason could be that in specimens with longer bond length, and GFRP bars will tolerate more stress and debonded along with the concrete cover. For example, an increase in NSM bar bond length from 800 to 1300 mm with concrete covers from 25 to 40 mm decreased the ductility index by 3% and 8%, respectively. The highest ductility index is related to the NSM–CFRP confinement combined method. Using CFRP wrap in specimens with 25- and 40-mm concrete covers, 26% and 10% increase ductility, respectively, compared to NSM-strengthened specimens. It is also concluded that CFRP

wrap effect on ductility enhancement is fewer when the concrete cover is more.

10 Energy Dissipation Capacity

Energy dissipation is an important factor in studying structures' behavior; when it is higher, the structure performance is better. The dissipated energy is found by computing area under the load–displacement diagram. Similar to the ductility index, the energy dissipation capacity of beams with more concrete cover is higher. NSM strengthening method with a bond length of 800 mm causes an increase of 125 and 155% in energy dissipation capacity in beams with 25- and 40-mm concrete cover, respectively. Adding CFRP confinement to NSM-strengthened specimens in beams with 25- and 40-mm concrete cover increases the energy dissipation capacity by 52 and 7%, respectively, indicating that in beams with lower concrete covers, CFRP confinement

effect is higher concerning enhancing the energy dissipation capacity. An increase in NSM bar bond length from 800 to 1300 mm will raise the energy dissipation capacity; in the beam with a 25-mm concrete cover, this increase is 29% and 25% for 40-mm cover. It means that the effect of increased NSM bar length with different concrete covers on increasing the energy dissipation capacity would be approximately similar.

11 Conclusions

This study investigated the effects of two strengthening methods on increasing the flexural strength of lap-spliced beams: (i) NSM with bond lengths of 800 and 1300 mm and (ii) NSM-CFRP confinement. A four-point bending test was applied on the beams where the results are briefly given as follows:

1. Compared to control specimens, strengthening methods (NSM and NSM-CFRP confinement) led to more load-bearing capacity, final displacement, ductility, and energy dissipation capacity of lap-spliced RC beams.
2. The specimens with longer NSM bar have lower ductility index than those of short NSM bar, while the flexural strength and energy dissipation capacity of beams with longer NSM bar are higher.
3. Adding CFRP confinement to lap-spliced RC beams strengthened by NSM method (NSM-CFRP confinement) increases ductility and energy dissipation capacity, while this confinement considerably causes a slight increase for load-bearing capacity.
4. The effects of strengthening methods on increasing the flexural strength of beams with more concrete covers are slightly higher. It should be noted that CFRP wrap effect on increasing the ductility and energy dissipation capacity would be lower, while concrete cover is more.

References

- ACI 440.3R (2004) Guide test methods for fiber-reinforced polymers (FRPs) for reinforcing or strengthening concrete structures. American Concrete Institute, Farmington Hills
- Allam SM (2013) Flexural strengthening of RC beam with lap splices. *Int Rev Civ Eng* 4(5):256–273
- Al-Mahmoud F, Castel A, Francois R, Tourneur C (2009) Strengthening of RC members with near-surface mounted CFRP rods. *Compos Struct* 91(2):138–147
- Al-Rousan RZ, Issa MA (2017) Flexural behavior of RC beams externally strengthened with CFRP composites exposed to severe environment conditions. *KSCE J Civ Eng* 21:2300–2309
- Anagnostou E, Rousakis TC, Karabinis AI (2019) Seismic retrofitting of damaged RC columns with lap-spliced bars using FRP sheets. *Compos Part B Eng* 166:598–612
- Bournas DA, Triantafillou TC (2011) Bond strength of lap-spliced bars in concrete confined with composite jackets. *ASCE J Compos Constr* 15(2):156–167
- Cohn MZ, Barlett M (1982) Computer-simulated flexure tests of partially prestressed concrete section. *ASCE J Compos Div* 108(12):2747–2765
- DIN EN 10002 (1991) Tensile testing of metallic materials—part 1: method of test at ambient temperature. DIN—Adopted European Standard
- ElGawady M, Endeshaw M, McLean D, Sack R (2010) Retrofitting of rectangular columns with deficient lap splices. *ASCE J Compos Constr* 14(1):22–35
- El-Hacha R, Rizkalla S (2004) Near-surface-mounted fiber-reinforced polymer reinforcements for flexural strengthening of concrete structures. *ACI Struct J* 101(5):717–726
- ElSouri AM, Harajli M (2011) Seismic repair and strengthening of lap splices in RC columns: carbon fiber-reinforced polymer versus steel confinement. *ASCE J Compos Constr* 15(5):721–731
- Fakharifar M, Dalvand A, Sharbatdar MK, Chen G, Sneed L (2016) Innovative hybrid reinforcement constituting conventional longitudinal steel and FRP stirrups for improved seismic strength and ductility of RC structures. *Front Struct Civ Eng* 10:44–62
- Garcia R, Helal Y, Pilakoutas K, Guadagnini M (2014) Bond behaviour of substandard splices in RC beams externally confined with CFRP. *Constr Build Mater* 50:340–351
- Garcia R, Helal Y, Pilakoutas K, Guadagnini M (2015) Bond strength of short lap splices in RC beams confined with steel stirrups or external CFRP. *Mater Struct* 48(1–2):277–293
- Garcia R, Guadagnini M, Pilakoutas K, Pech Poot LA (2017) FRP strengthening of substandard lap-spliced RC members: a comprehensive survey. *Adv Struct Eng* 20(6):976–1001
- Haddad RH, Almomani OA (2019) Flexural performance and failure modes of NSM CFRP-strengthened concrete beams: a parametric study. *Int J Civ Eng* 17(7):935–948
- Hamad BS, Rteil AA, Soudki KA (2004a) Bond strength of tension lap splices in high-strength concrete beams strengthened with glass fiber reinforced polymer wraps. *J Compos Constr* 8(1):14–21
- Hamad BS, Rteil AA, Salwan BR, Soudki KA (2004b) Behavior of bond-critical regions wrapped with fiber-reinforced Polymer sheets in normal and high-strength concrete. *J Compos Constr* 8(3):248–257
- Hashemi SH, Maghsoudi AA, Rahgozar R (2009) Bending response of HSRC beams strengthened with FRP sheets. *Sci Iran Trans A Civ Eng* 16(2):138–146
- Hassan T, Rizkalla S (2002) Flexural strengthening of prestressed bridge slabs with FRP systems. *PCI J* 47:76–93
- Hassan T, Rizkalla S (2003) Investigation of bond in concrete structures strengthened with near surface mounted carbon fiber reinforced polymer strips. *J Compos Constr* 7(3):248–257
- Kheyroddin A, Naderpour H, Ghodrati Amiri G, Hoseini Vaez SR (2011) Influence of carbon fiber reinforced polymers on upgrading shear behavior of RC coupling beams. *IJST Trans Civ Eng* 35(C2):155–169
- Lamanna AJ, Bank LC, Scott DW (2004) Flexural strengthening of reinforced concrete beams by mechanically attaching fiber-reinforced polymer strips. *ASCE J Compos Constr* 8(3):203–210
- Moodi Y, Farahi Shahri S, Mousavi SR (2017) Providing a model for estimating the compressive strength of square and rectangular columns confined with a variety of fibre-reinforced polymer sheets. *J Reinf Plast Compos* 36(21):1602–1612
- Moodi Y, Mousavi SR, Ghavidel A, Sohrabi MR, Rashki M (2018) Using response surface methodology and providing a modified model using whale algorithm for estimating the compressive

- strength of columns confined with FRP sheets. *Constr Build Mater* 183:163–170
- Moodi Y, Sohrabi MR, Mousavi SR (2020) Effects of stirrups in spliced region on the bond strength of corroded splices in reinforced concrete (RC) beams. *Constr Build Mater* 230:116873
- Mostofinejad D, Moghaddasi A (2014) Bond efficiency of EBR and EBROG methods in different flexural failure mechanisms of FRP strengthened RC beams. *Constr Build Mater* 54:605–614
- Nardone F, Lignola GP, Protà A, Manfredi G, Nanni A (2011) Modeling of flexural behavior of RC beams strengthened with mechanically fastened FRP strips. *Compos Struct* 93:1973–1985
- Obaidat YT, Ashteyat AM, Obaidat AT (2020) Performance of RC beam strengthened with NSM-CFRP strip under pure torsion: experimental and numerical study. *Int J Civ Eng* 18:585–593
- Siddika A, Al Mamun A, Alyousef R, Amran YHM (2019) Strengthening of reinforced concrete beams by using fiberreinforced polymer composites: a review. *J Build Eng* 25:100796
- Youm KS, Lee YH, Choi YM, Hwang YK, Kwon TG (2007) Seismic performance of lap-spliced columns with glass FRP. *Mag Concr Res* 59(3):198–198